JOURNAL OF SOLID STATE CHEMISTRY 36, 52–65 (1981)

# Crystallography and Phase Relations of $MeO$–$M_2O_3$–$TiO_2$ Systems ($Me$ = Fe, Mg, Ni; $M$ = Al, Cr, Fe)

J. HAUCK

*Institut für Festkörperforschung der Kernforschungsanlage, Jülich, D-5170 Jülich, Federal Republic of Germany*

Received December 31, 1979; in revised form March 31, 1980

Subsolidus phase relations of ternary oxide systems containing divalent Fe, Mg, or Ni, trivalent Al, Cr, or Fe, and tetravalent Ti are characterized by solid solutions at metal/oxygen ratios 3/4, 2/3, and 3/5. At low temperatures only compounds with cubic or hexagonal close-packed oxygen and uniform oxygen coordination remain stable in the crystal structures NaCl, spinel, ilmenite-$\alpha$-$Al_2O_3$, $TiO_2$. The pseudobrookite phases $FeTi_2O_5$, $MgTi_2O_5$, $Al_2TiO_5$, $Fe_2TiO_5$, the $V_3O_5$ structure phase $Cr_2TiO_5$, and the Andersson phases $Cr_2Ti_{n-2}O_{2n-1}$ ($n$ = 4,6,7,8,9) decompose. Additional phases with close-packed oxygen as predicted by a simple structure model for metal/oxygen ratios 7/12, 5/6, and 11/12 do not form but presumably are important for nonstoichiometric solid solutions. Most differences between systems containing transition metals and the $MgO$–$Al_2O_3$–$TiO_2$ system can be attributed to crystal field effects.

## I. Introduction

Ternary oxide systems $MeO$–$M_2O_3$–$TiO_2$ with divalent $Me$ = Fe or Mg, trivalent $M$ = Al or Cr, and tetravalent Ti have been investigated to study petrogenesis of the opaque phases in lunar rocks (*1–3*). Basalts from Mare Serenitatis and Mare Tranquillitatis contain up to 14 wt% $TiO_2$ with the bulk concentrated in ilmenite (Fe, Mg)$TiO_3$ (with some $Al_2O_3$ and $Cr_2O_3$ in solid solution), spinel (Fe, Mg)$_2TiO_4$–(Fe, Mg)(Al, Cr)$_2O_4$ss, and the new mineral armalcolite (Fe, Mg)$Ti_2O_5$.

From a crystallographic point of view the ternary systems $MeO$–$M_2O_3$–$TiO_2$ can be considered to be a good example for discussion of the distribution of di-, tri-, and tetravalent metal atoms at tetrahedral or octahedral interstices of close-packed oxygen layers. The octahedral ionic radii (*4*) of the metal atoms—including also $Ni^{2+}$ and $Fe^{3+}$ in this investigation—increase in the series $Al^{3+}$ (0.530) < $Ti^{4+}$ (0.605) < $Cr^{3+}$ (0.615) < $Fe^{3+}$ (0.645) < $Ni^{2+}$ (0.700) < $Mg^{2+}$ (0.720) < $Fe^{2+}$ (0.770 Å) and are close to the lower limit for octahedral coordination (0.58 Å). Tetrahedral coordination frequently occurs for $Al^{3+}$, $Mg^{2+}$, $Fe^{2+}$, and $Fe^{3+}$. $Ni^{2+}$ and $Cr^{3+}$ prefer octahedral coordination due to strong crystal field stabilization energy, which is 0.84 $\Delta$oct compared to 0.13 $\Delta$oct for $Ti^{3+}$ and $Fe^{2+}$ or 0 for $Fe^{3+}$ (and $Mg^{2+}$, $Al^{3+}$) for high spin state, and the relation $\Delta$tet = 4/9 $\Delta$oct between tetrahedral and octahedral crystal field splitting (*5, 6*). The influence of crystal field stabilization energy and of size effects on thermodynamic properties can be studied by comparison of phase relations within different ternary systems $MeO$–$M_2O_3$–$TiO_2$. The possible crystal structures for $Me$, $M$, or Ti

0022-4596/81/010052-14$02.00/0

atoms at tetrahedral or octahedral interstices are derived from a structure model.

## II. Structure Model

The structure model of this investigation is based on the assumption that structures with cubic or hexagonal close-packed oxygen layers (ccp or hcp) are preferred by ternary oxides with small metal atoms, which can be placed at tetrahedral or octahedral interstices. For hcp and ccp the most economical use is made of space and the highest symmetry can be achieved (*7*). Any other sequence of layers will have a lower symmetry. A model considering the coordination polyhedra of interstitial sites around the oxygen atoms of ccp and hcp (Fig. 1) and Pauling's electrovalence rule can be applied to derive theoretical structures, as was performed for ternary oxide systems containing $Li^+$ (*8*). The positions of tetrahedral and octahedral interstices near the oxygen atoms are indicated by letters a–h and numbers 1–6, respectively. They can be occupied by di-, tri-, and tetravalent metal atoms, if the following rules are regarded:

(1) For the overall composition, the sum of the metal atom charges must equal the sum of the oxygen atom charges because of the electroneutrality of the compound.

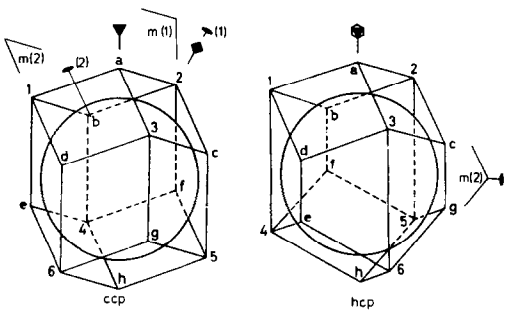


FIG. 1. Interstitial sites nearby an oxygen atom of ccp or hcp for tetrahedral (letters) or octahedral (numbers) coordinated metal atoms and some symmetry elements at the oxygen atom.

(2) Pauling's electrovalence rule requires a compensation of the metal atom charges in the neighborhood of each oxygen atom. The metal atoms with the charge $z$ and the coordination number $n$ contribute the electrovalence $z/n$ to the oxygen atom. The sum of the electrovalencies should equal the formal charge 2 of oxygen.

$$\Sigma\, z/n = 2\ (\pm\tfrac{1}{8}).$$

This rule can also be interpreted as that the smallest building blocks of the structure have as far as possible a composition identical with the overall composition of the compound (*8*, *9*). A deviation of $\frac{1}{8}$ is within the limit of this rule. For arrangements of metal atoms with a positive deviation, the electroneutrality rule requires another kind of oxygen surrounding with the same negative deviation. In this investigation, values with deviations from Pauling's rule are considered only if both oxygen atoms have the same number of metal atoms at octahedral and tetrahedral interstices.

(3) In an undistorted hcp packing with an O–O distance of 2.9 Å, neighboring tetrahedral sites (d–e, b–f, c–g) are 1.18A apart. Octahedral and tetrahedral sites 1-a, 2-c, etc., in hcp or ccp are at 1.78 Å. These sites will not be occupied simultaneously by atoms with ionic radii of ~0.6 Å, in the latter case, especially not by more highly charged metal atoms, because of Coulomb repulsion at short distance. The tetrahedral positions a and h can both be occupied only if all octahedral positions are vacant, because of the same distance restrictions applied to oxygen atoms of neighboring layers.

All structural arrangements obtained by this structure model are listed in Table I. The site symmetries (if higher than 1) are derived for single oxygen atoms and compared with the known structures. They are decreased, if the coordination polyhedra are distorted or if the polyhedra of neighboring oxygen atoms exhibit different ori-

TABLE I

SITE SYMMETRY OF OXYGEN (OR OTHER ANIONS) AT OCCUPATIONS OF DIFFERENT NEIGHBORING TETRAHEDRAL AND OCTAHEDRAL SITES[a]

| Site symmetry | ccp | hcp |
|---|---|---|
| $m3m$ | (1–6; MgO) | |
| $\bar{4}3m$ | (a,e,f,g; ZnS) | |
| $\bar{6}m2$ | | (1–6; γ-$CNb_2$/L3′; (NiAs)), a,h) |
| $\bar{3}m$ | (a,h; ($OCu_2$)) | |
| $3m$ | (1,2,3; $CdCl_2$; ($Co_2(OH)_3Cl$); ($Cu_2(OH)_3Cl$)), (h,1,2,3; $MgAl_2O_4$; $GeNi_2O_4$), (b,c,d; (β-$Ag_2HgI_4$); (β-$Cu_2HgI_4$)), (a,b,c,d) | (1,2,3; $CdI_2$; ζ-$CNb_2$); (h,1,2,3; ($Al_2BeO_4$)), (e,f,g), (e,f,g,h), (a,e,f,g; ZnO) |
| $4/mmm$ | (1,3,4,5) | |
| $4mm$ | (1–5), (a,b,c,f; OPb) | |
| $mm2(1)$ | (1,2,5; anatase), (a,f,6), (a,f; $HgI_2$; (α-$ZnCl_2$)) | (2,3,5,6) |
| $mm2(2)$ | (1,2,3,6), (a,d,4,5) (a,d,f,h; SPt) (a,d; ($SiS_2$)) | |
| $m(1)$ | (a,4,5), (a,b,c,6), (a,b,c), (a,d,h), (a,b,c,h) | |
| $m(2)$ | (a,d,4) | (2–6; ($Cr_5S_6$)), (1,2,3,4; ($LiSbO_3$); ($Cr_2S_3$)), (g,1,2,3,4), (2,3,4; rutile; $CaCl_2$; AlO(OH); (α-$PbO_2$); ($NiWO_4$); ε-; (ζ-$NFe_2$); (ζ-$CNb_2$)), (g,2,3,4;$Al_2BeO_4$), (g,1,2,3), (e,f,1,2,3), (g,h,1,2,3), (g,2,3), (g,1,4), (h,2,3), (e,f,2,3), (g,h,2,3), (c,h,1,4), (c,h,1), (g,h,1), (e,f,1), (e,f,h,1), (c,e,f,1), (e,f,g,1), (a,g; (β-$ZnCl_2$)), (e,f; β-$ZnCl_2$), (a,c), (e,f,h), (a,e,f), (c,e,f), (a,c,h) |
| 2 | | (1,2,4,6; α-$Al_2O_3$; $LiSbO_3$), (b,e,3,5), (b,e; (β-$ZnCl_2$)) (a,b,e,h) |

[a] Indicated by letters a–h and numbers 1–6 (Fig. 1). Crystal structures are correlated to the configurations. Their formulas are given in brackets, if the site symmetry of the anion is lowered. In PbO, PtS, $Cu_2O$, $Nb_2C$, and $Fe_2N$ the metal atoms exhibit hcp or ccp. Two different twofold axes and mirror planes exist for $mm2$ and $m$ symmetry in ccp (Fig. 1). The site symmetry of O in rutile is increased to $mm2$ (7).

entations or different occupations with metal atoms, which is indicated by brackets. Crystal structures with configurations of low symmetry are less frequent probably because of some difficulty for a three-dimensional arrangement of the polyhedra. Table II shows the resulting composition of the oxides, if a certain fraction of octahedral and tetrahedral sites is occupied. Solid-solution phases with equal metal/oxygen ratios are indicated by numbers as shown in Fig. 2. Certain compositions of the solid solutions, where superstructures can be expected, are marked by letters in addition. For most compositions different structures are possible (Table II). The arrangements of metal atoms as obtained in the present investigation are doubly underlined. They belong to the following crystal structures: NaCl (phase **1**),[1] spinel (**2**), ilmenite-α-$Al_2O_3$ (**3**) and rutile (**5**). These are crystal structures with zero or one tetrahedral site besides the octahedral sites occupied. For the composition $Me_2TiO_4$ (**2a**) tetravalent Ti at tetrahedral sites is less favorable than divalent *Me*. In $Ni_2GeO_4$ tetravalent Ge occupies tetrahedral sites (*10*). In some other systems

[1] The phase numbers in the text are given by bold type.

TABLE II

OCCUPANCY OF TETRAHEDRAL AND OCTAHEDRAL SITES OF THE POLYHEDRA OF FIG. 1[a]

| Atoms at tet. site | Number of octahedral sites occupied | | | | | | |
|---|---|---|---|---|---|---|---|
| | 0 | 1 | 2 | 3 | 4 | 5 | 6 |
| — | — | — | — | 5 | 3a–e | 10a–c | 1 |
| *Me* | — | — | — | 2a–d | 11a,b | — | — |
| *M* | — | — | 9c | 2c,d | — | — | — |
| Ti | — | — | 9a–c | 2a | — | — | — |
| *MeMe* | — | — | 10a–c | 1 | — | — | — |
| *MeM* | — | — | 10c | — | — | — | — |
| *MM* | — | 3d,e | — | — | — | — | — |
| *Me*Ti | — | 3a,b | — | — | — | — | — |
| *MeMeMe* | — | 11a,b | — | — | — | — | — |
| TiTi | 5 | — | — | — | — | — | — |
| *MeMM* | 2d | — | — | — | — | — | — |
| *MeMe*Ti | 2a | — | — | — | — | — | — |
| *MeMeMeMe* | 1 | — | — | — | — | — | — |

[a] The composition of the phases as indicated by numbers and letters is shown in the phase diagram of Fig. 2. Configurations observed in phases of the $MeO$–$M_2O_3$–$TiO_2$ systems are double underlined, those assumed for nonstoichiometric solid solutions of those phases are dashed. Single-underlined values are known for other systems. Oxygen atoms with different combinations of *Me*, *M*, and Ti atoms at tetrahedral sites can occur at compositions **2e**, **2f**, **3f**, **3g**, **9d**, **10c**, and **10d**.

structures with metal atoms only at tetrahedral sites (single underlined) become stable (*11, 12*). A comparison of theoretical and observed structures in Table II suggests that simultaneous occupations of tetrahedral and octahedral sites are less favorable in close-packed structures. One reason for this might be the low symmetry of most configurations.

Additional theoretical phases derived by the structure model would have the metal/oxygen ratio 7/12 (phase **9**), 5/6 (phase **10**) and 11/12 (phase **11**). For those compositions, arrangements of metal atoms close to that of existing phases are possible (dashed underlined). Therefore, these configurations might have some importance for the nonstoichiometric solid solutions, which are up to ~5 wt% at the higher temperatures (*1*). The nonstoichiometric solid solutions are not shown in the phase diagrams of this investigation because of more complexity and some difficulty in determination at the lower temperatures. A nonstoichiometric solid solution versus the composition (**10a–c**) occurs, if one additional octahedral site of phase (**3a–e**) (ilmenite-$\alpha$-$Al_2O_3$) is occupied or if one octahedral site of phase (**1**) (NaCl structure) is vacant. A limited solid solution of ilmenite-$\alpha$-$Al_2O_3$ (**3a–e**) toward phase (**11a,b**) is obtained, if an additional tetrahedral site is occupied by *Me*. For the inverse spinel with composition (**2c,d**), a nonstoichiometric solid solution toward

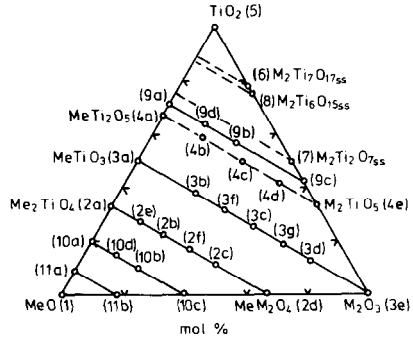


FIG. 2. Theoretical phase diagram $MeO$–$M_2O_3$–$TiO_2$ containing solid solutions of phases with close-packed oxygen atoms at metal/oxygen ratios 1/1 (phase **1**), 3/4 (phase **2**), 2/3 (phase **3**), 1/2 (phase **5**), 7/12 (phase **9**), 5/6 (phase **10**), and 11/12 (phase **11**). Superstructures can be expected at the composition $Me_2TiO_4$ (**2a**), $Me_5M_2Ti_2O_{12}$ (**2b**), $Me_4M_4TiO_{12}$ (**2c**), $MeM_2O_4$ (**2d**), $Me_{11}M_2Ti_5O_{24}$ (**2e**), $Me_3M_2TiO_8$ (**2f**), $MeTiO_3$ (**3a**), $Me_3M_2Ti_3O_{12}$ (**3b**), $MeM_2TiO_6$ (**3c**), $MeM_6TiO_{12}$ (**3d**), $M_2O_3$ (**3e**), $Me_5M_6Ti_5O_{24}$ (**3f**), $Me_3M_{10}Ti_3O_{24}$ (**3g**), $MeTi_2O_5$ (**4a**), $Me_3M_2Ti_7O_{20}$ (**4b**), $MeM_2Ti_3O_{10}$ (**4c**), $MeM_6Ti_5O_{20}$ (**4d**), $M_2TiO_5$ (**4e**), $Me_2Ti_5O_{12}$ (**9a**), $MeM_2Ti_4O_{12}$ (**9b**), $M_4Ti_3O_{12}$ (**9c**), $Me_3M_2Ti_9O_{24}$ (**9d**), $Me_4TiO_6$ (**10a**), $Me_7M_2TiO_{12}$ (**10b**), $Me_3M_2O_6$ (**10c**), $Me_{15}M_2Ti_3O_{24}$ (**10d**), $Me_{10}TiO_{12}$ (**11a**), $Me_9M_2O_{12}$ (**11b**). Solid solutions of the high-temperatures phases (**4**), (**6**), (**7**), and (**8**) are shown by dashed lines.

$M_4Ti_3O_{12}$ (**9c**) can be considered, if one octahedral position nearby some oxygen atoms is not occupied.

Ordered compounds with different coordination numbers of the oxygen atoms were reported for $M_2Ti_{n-2}O_{2n-1}$, $n$ = 3–9 and 15–~36 with the more covalent trivalent transition metals $M$ = Cr, Fe, and Ti (13–16) and are also known, e.g., for the less ionic sulfides $Cr_5S_8$, $Fe_7S_8$, $Cr_3S_4$, and $In_2S_3$ (*7*, *12*). The oxygen or sulfur atoms of those compounds exhibit a low site symmetry. The oxides of the present investigation with mixed oxygen coordination decompose at low temperatures as is described in Section IV. A separation into two phases with uniform oxygen coordination in each phase seems to be more favorable for stable low-temperature phases with strong Coulomb interactions.

## III. Phases with hcp or ccp Structures

Phase (**2**) is reported to be a normal spinel $Me[M_2]O_4$ with $Me$ = Mg or Fe at tetrahedral and $M$ = Al or Cr at octahedral interstices (*10*). $NiAl_2O_4$ is a 75% inverse spinel and $(Fe, Mg)_2TiO_4$ a 100% inverse spinel according to the formula $Ni_{1/4}Al_{3/4}[Ni_{3/4}Al_{5/4}]O_4$ and (Fe, Mg) [(Fe, Mg)Ti]$O_4$ with 25 or 50% of divalent $Me$ at tetrahedral sites. The inverse spinel character of $NiAl_2O_4$ and also of $Fe_3O_4$ and $NiFe_2O_4$ can be explained by the higher crystal field stabilization energy for $Ni^{2+}$ or $Fe^{2+}$ at octahedral sites (*5*, *6*, *10*). $NiCr_2O_4$ is a normal spinel with a tetragonal distorted hausmannite structure (*10*). $Ni^{2+}$ at tetrahedral sites gains crystal field energy by the tetragonal Jahn–Teller distortion. The $(Fe, Mg)_2TiO_4$ spinels exhibit a higher Coulomb energy if tetravalent Ti occupies octahedral interstices (*7*). At very low temperatures the Ti and Fe (or Mg) atoms should order at the octahedral interstices or the inverse spinels become unstable because of the remaining entropy. For the same reason only compositions given in Fig. 2 for the solid-solution series can stay stable in ordered low-temperature phases. The change of ordering in spinels can be without phase transition or first or second order (*17*). The change normal–statistical–inverse or normal–inverse in the solid solutions $MeM_2O_4$–$Me_2TiO_4$ can be first order or without phase transition. An ordering with two different atoms at tetrahedral sites, such as $Me$ and Ti in a theoretical structure of a spinel with the composition (**2e**) or (**2f**), could be accomplished by a first- or a second-order phase transition. Most of the other phase transitions can only be first order (*17*) but probably occur only at very low temperatures. The ordering of $Fe^{2+}$ and $Fe^{3+}$, e.g., at the octahedral interstices of the inverse spinel $Fe_3O_4$ = $Fe^{3+}[Fe^{2+}Fe^{3+}]O_4$ with a reduction of site symmetry of oxygen to $m$, was observed below 120 K (*17*). In this investigation no phase transition could be detected. In some systems, however, this would have been scarcely detectable by X-rays, because of the small difference in scattering power for neighboring elements (Mg, Al) or (Ti, Cr, Fe, Ni).

In $Cr_2O_3$–$NiTiO_3$ solid solution a phase transition between the structure of $Cr_2O_3$ (space group $R\bar{3}c$) and $NiTiO_3$ ($R\bar{3}$) (*11*) should occur with a reduction of site symmetry of oxygen atoms from 2 to 1, when the four metal atoms near each oxygen atom become ordered with a successive replacement of Cr by Ni and Ti at the compositions (**3b–d**). This measurement was not possible by X rays because of the similarity in scattering power of Ni, Cr, and Ti.

## IV. Phases Not Described by the Structure Model

Some phases of $MeO$–$M_2O_3$–$TiO_2$ systems with mixed oxygen coordination or

TABLE III

INFLUENCES OF SOLID-STATE REACTIONS AT DECREASING TEMPERATURES BY CRYSTAL FIELD STABILIZATION ENERGY $\Delta H_{CFS}$ IN DIFFERENT SYSTEMS[a]

| Reaction | Reaction product at $\Delta H_{CFS} \geq 0$ | Examples | Reaction product at $\Delta H_{CFS} < 0$ | Examples | $\Delta H_{CFS}$ |
|---|---|---|---|---|---|
| a | $Me[M_2]O_4$(2d) | $MgAl_2O_4$, $MgFe_2O_4$, $MgCr_2O_4$, $FeCr_2O_4$, $NiCr_2O_4$ | $M[MeM]O_4$(2d) | $(FeAl_2O_4)$, $Fe_3O_4$, $NiAl_2O_4$, $NiFe_2O_4$ | $-H_{Me} + H_M$ |
| b | | | $[Me]O(1) + [M_2]O_3$(3e) | — | $-H_{Me}$ |
| c | $Me[MeTi]O_4$(2a) | $Mg_2TiO_4$ | $Ti[Me_2]O_4$(2a) | — | $-H_{Me}$ |
| d | | | $[Me]O(1) + [MeTi]O_3$(3a) | $Fe_2TiO_4$?, $Ni_2TiO_4$ | |
| e | $MeTi[Ti]O_5$(4a) | $MgTi_2O_5$ | $[MeTi]O_3$(3a) + $[Ti]O_2$(5) | $FeTi_2O_5$, $NiTi_2O_5$ | $-H_{Me}$ |
| f | $M_2[Ti]O_5$(4e) | $Al_2TiO_5$, $Fe_2TiO_5$ | $[M_2]O_3$(3e) + $[Ti]O_2$(5) | $Cr_2TiO_5$ | $-2H_M$ |
| g | | | $[M_2Ti]O_5$(4e) | | |
| h | $Me[M_2]O_4$(2d) + 3$[Ti]O_2$(5) | MAT, MCT, MFT?, FCT | $MeM_2Ti[Ti_2]O_{10}$(4c) | — | $+2H_M$ |
| i | $M[MeM]O_4$(2d) 3$[Ti]O_2$(5) | FFT?, NAT, NFT? | | — | $+H_{Me} + H_M$ |
| j | $Me[M_2]O_4$(2d) + $[Ti]O_2$(5) | MAT, MCT, MFT? | $[MeM_2Ti]O_6$(3c) or $[MeTi]O_3$(3a) + $[M_2]O_3$(3e) | FAT, (FCT), NCT | $-H_{Me}$ |
| k | $M[MeM]O_4$(2d) + $[Ti]O_2$(5) | FFT?, NAT, NFT? | | — | $-H_M$ |
| l | $2Me[M_2]O_4$(2d) + $2MeTi[Ti]O_5$(4a) | MAT, MCT, MFT?, FCT | $Me_2[MeM_2Ti]O_6$(2f) + $MeM_2Ti[Ti_2]O_{10}$(4c) | FAT | $-H_{Me} + 2H_M$ |
| m | $2M[MeM]O_4$(2d) + $2MeTi[Ti]O_5$(4a) | FFT?, NAT, NFT? | $MeM[Me_2MTi]O_6$(2f) + $MeM_2Ti[Ti_2]O_{10}$(4c) | — | $+H_M$ |
| n | $Me[M_2]O_4$(2d) + $[MeTi]O_3$(3a) | MAT, MCT, MFT?, FAT, FCT, NCT | $Me[MeTi]O_4$(2a) + $[M_2]O_3$(3e) | — | 0 |
| o | $M[MeM]O_4$(2d) + $[MeTi]O_3$(3a) | FFT?, NAT, NFT? | | — | $H_{Me} - H_M$ |
| p | $[Me_3M_2Ti_3]O_{12}$(3b) + $4MeTi[Ti]O_5$(4a) | MAT, MCT, MFT?, FCT | $4[MeTi]O_3$(3a) + $Me_3M_2Ti_3[Ti_4]O_{20}$(4b) | FAT, FFT?, NAT, NFT? | $-H_{Me} + 2H_M$ |
| q | $MeM_2Ti[Ti_2]O_{10}$(4c) + $(2n - 6)[Ti]O_2$(5) | MAT | $[MeM_2Ti_3]O_{10} \cdot (2n - 6)[Ti]O_2$ (4c, 6ss, 7ss, 8ss etc.) | MCT, FAT, FCT, NAT?, NCT | $-H_{Me} - 2H_M$ |

[a] Exceptions are given in brackets.

with strong deviations from hcp or ccp are shown in Fig. 2 by dashed lines. At the metal/oxygen ratio 3/5 phase (**4**) with pseudobrookite or $V_3O_5$ structure is formed, both of which can be related to ilmenite-$\alpha$-$Al_2O_3$ and rutile structures (*11, 16*). In the pseudobrookite structure $TiO_6$ octahedra are linked to $\infty[TiO_5]$ chains and *M* atoms of $M_2TiO_5$ or *Me* and the second Ti atom of $MeTi_2O_5$ are at approximately tetrahedral coordination with two additional oxygen atoms of a greater distance. Their coordination can change from tetrahedral to octahedral by variation of *xyz* parameters. Pauling's rule would be violated for undistorted octahedra with three or four nearest metal atoms of the O atoms. The $V_3O_5$ structure is built up of $VO_6$ octahedra which are mutually joined by sharing corners, edges, and faces. Some oxygen atoms of distorted hcp have three nearest metal atom neighbors similar to rutile; others exhibit four neighbors as in ilmenite structure. The phases with high Cr content prefer the $V_3O_5$ structure because of the high octahedral crystal field stabilization of $Cr^{3+}$. The phases decompose at low temperatures: $Fe_2TiO_5$ below 585°C (*18*), $Al_2TiO_5$ below 1286°C, $Cr_2TiO_5$ below 1660°C (*19*), pure $FeTi_2O_5$ below 1140°C (*18*), $MgTi_2O_5$ below 620°C (*20*), or 720°C as obtained by a hydrothermal run at 2.7 kb argon pressure in this investigation. At high pressure the phases of pseudobrookite structure type decompose at higher temperatures because of the larger volume compared to decomposition products with hcp or ccp structures as was shown, e.g., by the decomposition of $MgTi_2O_5$ to $MgTiO_3$ and $TiO_2$ (*20*).

Phases (**6**), (**7**), and (**8**) are Andersson phases of the series $Cr_2Ti_{n-2}O_{2n-1}$ with $n$ = 4–9, which are closely related to rutile or $\alpha$-$PbO_2$ structure (at $n$ = 4) with crystallographic shear planes, where octahedra are linked by faces as in $\alpha$-$Al_2O_3$ (*13, 14*). Three oxygen atoms of one formula unit exhibit the coordination number 4; the other, that of three nearest metal atoms. There are alternating layers of different composition or to some extent also a disordered sequence of layers in nonstoichiometric solid solutions (*19*) between $TiO_2$ and the nonexisting $Cr_4Ti_3O_{12}$ (**9c**). A $Cr_4Ti_3O_{12}$ would contain equal numbers of oxygen atoms with one Cr and two Ti or three Cr and one Ti atoms as nearest neighbors. These phases become unstable at low temperatures, which, however, is difficult to achieve because of kinetic problems. The following decomposition temperatures were obtained in this investigation by use of a small amount of a potassium-tetraborate-10 wt% PbO flux: $Cr_2Ti_2O_7$ (phase E or **7**) (~1205°C), $Cr_2Ti_4O_{11}$ (1420°C), $Cr_2Ti_5O_{13}$ (1340°C), $Cr_2Ti_6O_{15}$ (phase **8**) (~1280°C), $Cr_2Ti_7O_{17ss}$ (phase **6**) (~1250°C). At higher temperatures with that flux the phases stayed unchanged. The decomposition temperatures of $Cr_2Ti_4O_{11}$ and $Cr_2Ti_5O_{13}$ are in good agreement with former results without flux (*19*). Similar phases are reported for systems with trivalent Fe at temperatures above 1450°C and are probably stabilized by divalent Fe at lower temperatures (*14, 15*).

In the oxide systems of this investigation only compounds with close-packed oxygen layers and uniform coordination of the oxygen atoms remain at low temperatures. Their structures can be described by the structure model of Section II.

## V. Relations between Structural and Thermodynamic Properties

The relations between structural and thermodynamic properties could be discussed, if phase diagrams at very low temperatures were obtained. At low temperatures the metal atoms become ordered at the interstitial sites and the solid solutions are restricted to the compositions of those

ordered compounds. The configurations of the metal atoms at the interstices are mainly determined by Coulomb interactions. In this investigation, equilibrium of prereacted oxide mixtures could be obtained only at temperatures above about 900–1300°C, depending on composition, and also in a few runs at lower temperatures by use of a flux or in hydrothermal reactions. Because of the kinetic problems at low temperatures the phase relations were studied over a larger temperature range to obtain some idea of how the system develops at decreasing temperatures. For each system two typical isothermal sections are shown in Fig. 3 and phase relations are discussed in detail in the next section. For FeO-containing systems, phase relations were also studied at different oxygen partial pressures: in contact with metallic iron, at reducing conditions of $H_2/CO_2$ gas mixtures in different ratios, and in air. The isobaric 1000 and 1300°C sections (Fig. 4) were derived from these experiments and from literature data for $FeO_x$–$TiO_2$ and $FeO_x$–$Al_2O_3$ systems (*21, 22*). At higher oxygen partial pressures divalent Fe is oxidized to the trivalent state. At strongly reducing conditions, some $Ti^{3+}$ can occur, especially in ferropseudobrookite phase $FeTi_2O_5$–$Ti_3O_{5ss}$ and ilmenite phase $FeTiO_3$–$Ti_2O_{3ss}$ (*20, 23*).

The change of phase relations and in particular of conjugation lines between coexisting phases with decreasing temperatures or at different oxygen partial pressures (in FeO-containing systems) can give some indication of the stability of a compound. The variation of conjugation lines between coexisting phases A and B at high temperatures to A and C at low temperatures can be explained by increasing thermodynamic stability of phase C compared to phase B at low temperatures. B and C can be phases with different structures or only different compositions of a solid solution. A variation of the conjugation lines to a certain composition of a solid solution can mean that this particular composition becomes ordered and thereby more stable than the disordered solid solution. The lattice constants change discontinuously at a miscibility gap and quite often exhibit a

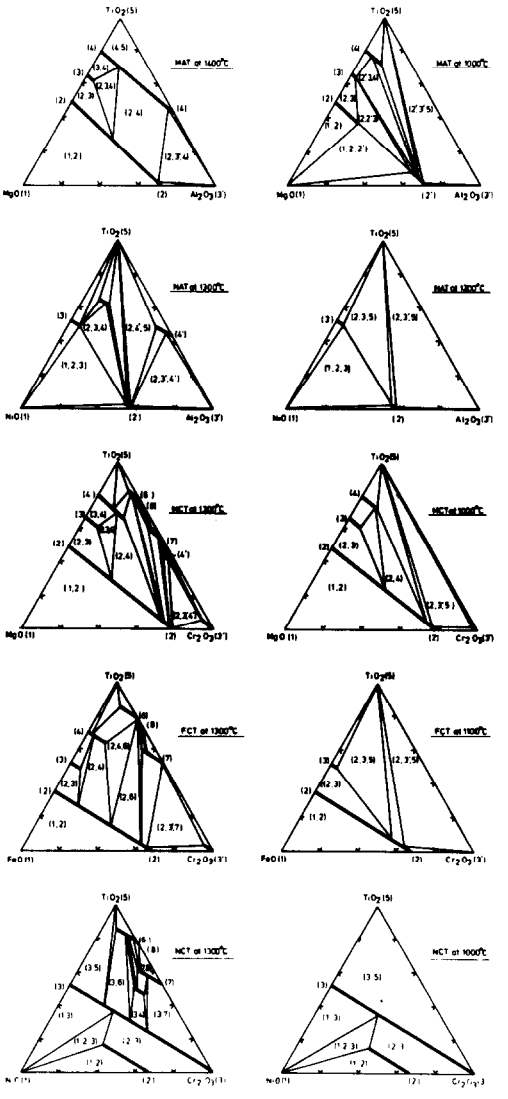

FIG. 3. Isothermal sections of $MeO$–$M_2O_3$–$TiO_2$ systems at two different temperatures. The phases are given by numbers as shown in Fig. 2 (compositions in wt%).

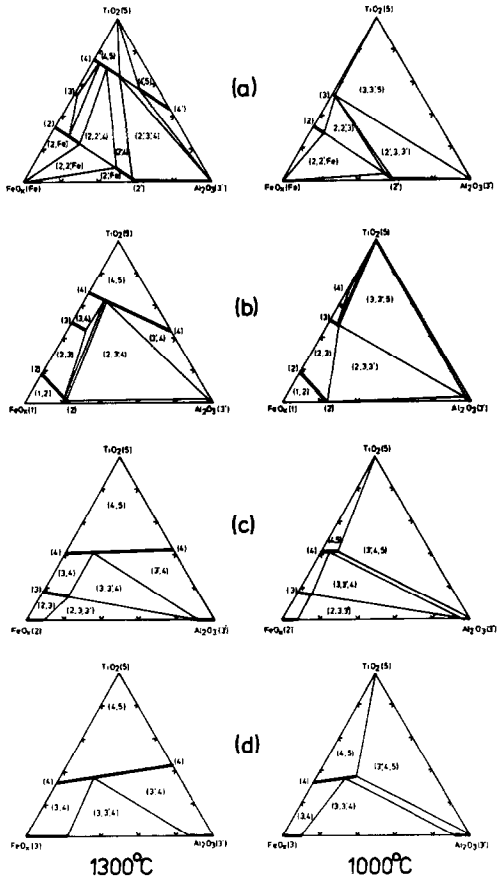


FIG. 4. Phase relations of $FeO_x$–$Al_2O_3$–$TiO_2$ system in wt% for different oxygen partial pressures $p(O_2)$ at 1300 and 1000°C, respectively: (a) in contact with Fe; (b) $-\log p(O_2) = 8.5$ and ~14.0, respectively; (c) 2.5 and ~6.0; (d) 0.7 for both temperatures.

deviation from Vegard's rule, if an intermediate composition becomes ordered.

## VI. Phase Relations in $MeO$–$M_2O_3$–$TiO_2$ Systems

### *$MgO$–$Al_2O_3$–$TiO_2$ (MAT) System*

The MAT system contains phases (1–5). The spinel (phase 2) forms a solid solution with a miscibility gap at 63 mole% $MgAl_2O_4$ below ~1370°C (*1*). The lattice constants decrease nearly linearly from $Mg_2TiO_4$ to $MgAl_2O_4$ with a small negative deviation at 60–100 mole% $MgAl_2O_4$ (*1*). The pseudobrookite solid solution (phase 4) is complete above ~1286°C. There are two miscibility gaps at ~50 and 100 mole% $Al_2TiO_5$. At 1170°C, some solid solution with about 65 mole% $Al_2TiO_5$ is still stable but has decomposed at 1100°C. The larger lattice constants of the orthorhombic unit cell decrease linearly from $MgTi_2O_5$ to $Al_2TiO_5$; the smallest one exhibits a small negative deviation from Vegard's rule. At 1400°C, $MgTiO_3$ and $Al_2O_3$ (phases 3 and 3′) form very limited solid solutions, which do not coexist. At decreasing temperature the three phase triangles (2, 3, 4) and (2, 3′, 4) turn in a counterclockwise direction. The stability of spinel (2) increases with respect to the normal spinel $MgAl_2O_4$, whereas the stability of the pseudobrookite phase (4) decreases with increasing $Al_2TiO_5$ content. At 1000°C, $TiO_2$ is in equilibrium with a spinel of high $MgAl_2O_4$ content.

### *$FeO$ ($Fe_2O_3$)–$Al_2O_3$–$TiO_2$ (FAT) System*

In the FAT system, the influence of $Al_2O_3$ on the phase relations of the known system FeO–$Fe_2O_3$–$TiO_2$ (*21*) was studied. In the FeO–$Fe_2O_3$–$TiO_2$ system, the phases $Fe_2TiO_4$, $FeTiO_3$, and $FeTi_2O_5$ with divalent iron form complete solid solutions with the phases $Fe_3O_4$, $Fe_2O_3$, and $Fe_2TiO_5$, respectively, containing trivalent iron (phases 2, 3, and 4 of Fig. 2). The $Fe^{2+}/Fe^{3+}$ content of the solid solutions is mainly determined by $TiO_2$ content, if the nonstoichiometric solid solutions are neglected, and can be projected at the FeO–$TiO_2$ join of the pseudoternary isothermal sections $FeO_x$–$Al_2O_3$–$TiO_2$ of Fig. 4. The $TiO_2$ content of pseudobrookite phase (4) decreases from 69.0 wt% in $FeTi_2O_5$ to 33.4 wt% in $Fe_2TiO_5$, for $FeTiO_3$–$Fe_2O_3$ solid solution (phase 3) from 52.7 wt% in $FeTiO_3$ to 0% in $Fe_2O_3$, and for spinel (phase 2) from 35.7 wt% in $Fe_2TiO_4$ to 0% in $Fe_3O_4$. At strongly reducing conditions (b), single phases were obtained at 68 wt% $TiO_2$ (phase 4), 50 wt% $TiO_2$ (3), and 18 wt% (2).

Therefore, most of the iron of phases (3) and (4) is in a divalent state. At condition (a) (in contact with metallic iron), also, most iron in spinel (2) is reduced to the divalent state, but phases (3) and (4) already have a higher $TiO_2$ content as calculated for divalent iron because of some $Ti_3O_5$ and $Ti_2O_3$ with trivalent Ti in solid solution (*23*). At reducing conditions stronger than that of the present investigation $Ti_3O_5 = Ti_2O_3 \cdot TiO_2$ can form a complete solid solution with $FeTi_2O_5$ above ~1350°C (*24*). At higher $TiO_2$ content Andersson phases $Ti_nO_{2n-1} = Ti_2O_3 \cdot (n-2)TiO_2$, $n$ = 4–8 with ~1 at% $Fe^{2+}$ were obtained at 1200°C (*25, 26*).

$Fe_2TiO_4$ and $FeAl_2O_4$ form a solid solution (phase 2) with a miscibility gap between ~40 and 70 mole% $FeAl_2O_4$ at the eutectic temperature of ~1350°C (*1*). The lattice constants show a small negative deviation from Vegard's rule (*1*). The pseudobrookite solid solution $FeTi_2O_5$–$Al_2TiO_5$ has a miscibility gap at ~60 mole% below ~1340°C. A solid solution with about 80 mole% $Al_2TiO_5$ remains stable at 1210°C, but has decomposed at 1180°C to the phase assemblage (3', 4, 5). At an increase of $Fe^{3+}$ content, the solid solution becomes complete at 1300°C. An increase of stability with $Fe^{3+}$ content is also indicated for the 1000°C isothermal sections by the increased $Al_2TiO_5$ content in solid solution and can be explained by the higher stability of $Fe_2TiO_5$ compared to that of $FeTi_2O_5$. The smaller orthorhombic lattice constants of $Fe_2TiO_5$ and $FeTi_2O_5$ decrease nearly linearly to $Al_2TiO_5$. The largest constant exhibits a positive deviation from Vegard's rule in both solid solutions. $FeTiO_3$ and $Al_2O_3$ form a very limited solid solution. It increases with increasing $Fe_2O_3$ content. The phases (3) and (3') coexist at all reducing conditions at 1000°C and at the conditions (c) and (d) at 1300°C. The $Al_2TiO_5$ content of phase (4) coexisting with (3) and (3') decreases with $Fe^{2+}$ content.

For high $Fe^{2+}$ content, phase (4) is decomposed at 1000°C and (3) and (3') reach equilibrium with $TiO_2$ (5). At 1300°C (diagram (a)), the phase assemblages (2, 4) and (2', 4) instead of (3, 3') are preferred. The three phase triangles (2, 3, 4) and (2', 3', 4) change slightly at decreasing temperatures, as in the MAT system, and disappear as the pseudobrookite phase (4) becomes unstable. Then they are replaced by the three-phase triangles (2, 2', 3) and (2', 3, 3'), as shown in the 1000°C isothermal section (a).

*$NiO$–$Al_2O_3$–$TiO_2$ (NAT) System*

$NiAl_2O_4$ (phase 2) has only a very limited solid solution with the unstable $Ni_2TiO_4$. The pseudobrookite phase (4) exhibits three miscibility gaps. Some solid solution with ~25 mole% $Al_2TiO_5$ remains at 1300°C and has decomposed at 1250°C. The solid solution at about 85 mole% $Al_2TiO_5$ decomposes about 50°C lower than pure $Al_2TiO_5$. $NiTiO_3$ (3) forms a very limited solid solution with $Al_2O_3$ (3').

*$MgO$–$Cr_2O_3$–$TiO_2$ (MCT) System*

The spinel (phase 2) forms a complete solid solution even at 1000°C. The lattice parameters exhibit a small negative deviation from Vegard's rule. As in the MAT system, $TiO_2$ (5) and $MgCr_2O_4$ (2) coexist at 1000°C instead of $MgTiO_3$ (3) and $Cr_2O_3$ (3'), which are only slightly soluble. The three-phase triangle (2, 3, 4) changes as in the MAT system. At 1300°C $MgTi_2O_5$–$Cr_2TiO_{5ss}$ (4) has two miscibility gaps with a remaining phase (4') of $V_3O_5$ structure type at about 78 mole% $Cr_2TiO_5$. Also, the Andersson phases $Cr_2Ti_7O_{17}$ (6) and $Cr_2Ti_2O_7$ (7) are stabilized to lower temperatures by some solid solutions with unstable $MeTi_8O_{17}$ and $MeTi_3O_7$ ($Me$ = Mg, Fe, Ni). Phase (6) changes to the high-temperature modification (*19*) at increased Mg content (or Ni, Fe content in NCT and FCT systems). These phase transitions are not shown in Fig. 3. At 1400°C, phases (4) and

(7) are more extended and coexist; at 1500°C, also, phase (4') coexists with (4).

*$FeO$–$Cr_2O_3$–$TiO_2$ (FCT) System*

The isothermal sections of the FCT system as shown in Fig. 3 are derived for strongly reducing conditions, where most Fe is in the divalent and most Ti in the tetravalent state. The FCT system behaves similarly to the FAT system at low $Cr_2O_3$ content and similarly to the MCT system at high $Cr_2O_3$ content. Spinel (phase 2) forms a complete solid solution. The solid solutions of $FeTiO_3$ (3)–$Cr_2O_3$ (3') and of $FeTi_2O_5$ (4) toward $Cr_2TiO_5$ are very limited at 1300°C. With decreasing temperatures the spinel composition of (2, 3, 4) phase assemblage changes to higher $FeCr_2O_4$ content. At 1100°C, $TiO_2$ (5) coexists with a spinel (2) of high $FeCr_2O_4$ content. A solid solution of $Ti_3O_5$ with trivalent Ti stabilizes phase (4) to lower temperatures and decreases the temperature for the appearance of the phase assemblage (2, 3, 5) to 1038°C (*27*).

*$NiO$–$Cr_2O_3$–$TiO_2$ (NCT) System*

In the NCT system $NiTiO_3$ and $Cr_2O_3$ form a complete solid solution (phase 3), and $NiCr_2O_4$ (2) forms a limited solid solution with unstable $Ni_2TiO_4$. Hydrothermal runs suggest that phase (3) exhibits a miscibility gap below ~1000°C. At 1300°C, a phase (4) of $V_3O_5$ structure type occurs at about 57 mole% $Cr_2TiO_5$ and the Andersson phases (6 and 7) show some solid solutions which are more extended than those in the MCT system. Phase (4) decomposes below ~1120°C.

## VII. Comparison of Phase Relations

The phase diagrams $MeO$–$M_2O_3$–$TiO_2$ can be characterized by the extent of solid solutions of phase (2, spinel), (3, ilmenite-$\alpha$-$Al_2O_3$), and (4, pseudobrookite or $V_3O_5$ structure). The miscibility gap of $Al_2O_3$-containing spinels (2) are approximately symmetric (*1*) as for regular disordered solid solutions with a slight shift to the more stable Al spinels. $Cr_2O_3$-containing spinels exhibit miscibility gaps at temperatures far below 1000°C as can be estimated from the system $MeAl_2O_4$–$MeCr_2O_4$–$Me_2TiO_4$ ($Me$ = Fe, Mg) (*1*). The strong temperature-dependent variation of the conjugation lines of phases coexisting with (2) suggest that there are no ordered phases with increased stability at intermediate compositions. At the lower temperatures, the conjugation lines approach composition (2d), which is the most stable spinel in those systems.

Extended solid solutions of phase (3) can be obtained in $FeO$–$Fe_2O_3$–$TiO_2$ (FFT) (*21*) and NCT systems and dissolve seemingly regularly below ~1000°C. In the NCT system, the three-phase triangles of coexisting phases do not approach one particular composition, as would have been expected, if this becomes ordered and thereby more stable. At 1000-~1500°C, the system $MgO$–$Fe_2O_3$–$TiO_2$ (MFT) (*28*) exhibits also some extended solid solution of phase (3) with a miscibility gap of coexisting phases (2, 4) similar to that in the MAT system at 1400°C (Fig. 3).

Phase (4) exhibits two miscibility gaps with the solid solution of 75 ± 10 mole% $M_2TiO_5$ in $MeTi_2O_5$ (4d) extending to lower temperatures. In the NAT system also the solid solution at the approximate composition (4b) extends to lower temperatures. This suggests that $M_2TiO_5$ with pseudobrookite or $V_3O_5$ structure has slightly increased stability, if one $Me$ atom (in the NAT system also three $Me$ atoms) is within the tetramolecular unit cells.

Some major differences in phase relation can be explained qualitatively by crystal field effects. This can be demonstrated by the different solid-state reactions of transition and non-transition metals in phases (2,

spinel) and (**4**, pseudobrookite) (Table III). In phases (**2**) and (**4**), only the parts of the metal atoms enclosed in square brackets are at octahedral interstices. Crystal field stabilization energy $\Delta H_{CFS}$ with the approximate values $H_{Fe} = 4$, $H_{Ni} = 22$, and $H_{Cr} = 42$ kcal/mole (*5*, *6*) can be gained in solid-state reactions, if the numbers of $Me$ = Fe, Ni or $M$ = Cr atoms at octahedral sites are increased. These reactions can be a structural change of a single phase (reactions a, c, and g), a decomposition of a phase (reactions b, d–f, h–k, and q), or a compositional change of coexisting phases (reaction 1-p). The different spinel solid solutions of two inverse spinels $Me[MeTi]O_4$–$M[MeM]O_4$ or of inverse and normal spinel $Me[MeTi]O_4$–$Me[M_2]O_4$ are both considered for reactions h–**0**. Phrase (*4*) with $V_3O_5$ structure is important for reactions (g) and (q) at very high temperatures. Only reactions strongly dependent on temperature are considered for crystal field effects. At decreasing temperatures the entropy becomes less important and the reactions are mainly governed by the reaction enthalpy. In that case the crystal field stabilization energy $\Delta H_{CFS}$ can influence a reaction, if it is large compared with other contributions to the reaction enthalpy such as different Coulomb interactions and different polarization energies. In some cases, as indicated by brackets, the crystal field is not strong enough to overrule other factors. The normal spinel $MgAl_2O_4$, e.g., obviously is stabilized by a larger enthalpy value, so that the small $H_{Fe}$ does not change the spinel character and the stronger $H_{Ni}$ cannot reach a complete inversion. Also, reaction (n) with $\Delta H_{CFS} = 0$ gives some indication for other factors influencing solid-state reactions in those systems. The reaction of coexisting phases is more shifted to the right side for $Cr_2O_3$ than $Al_2O_3$-containing systems. In $Al_2O_3$-containing systems the end members of phases (**2**) and (**3**) are more stabilized with respect to intermediate compositions, which can also be concluded from the reduced solid solutions.

In reaction (a), the stable normal spinel $MgAl_2O_4$ changes to the inverse spinel, if $\Delta H_{CFS} = -H_{Me} + H_M < 0$ (with the exception of $FeAl_2O_4$). The decomposition reaction (b) seems to be less favorable than the structural change. Spinels (**2a**) are less stable and prefer decomposition by reaction (d) for $Ni_2TiO_4$ and probably also for $Fe_2TiO_4$ at temperatures lower than that of the present investigation. Pseudobrookite (**4**) can decompose to the phase assemblage (**3**, **5**) in reactions (e) and (f) for the end members (**4a**, **4e**) or to (**2**, **5**) at the intermediate composition (**4c**) in reactions (h) and (i). The transition metal compounds with $Me$ = Fe, Ni and $M$ = Cr are less stable than the compounds $MgTi_2O_5$, $Al_2TiO_5$, and $Fe_2TiO_5$ and their solid solutions. In $Cr_2O_3$-containing systems, the formation (g) of a phase (**4**) of $V_3O_5$ structure type instead of decomposition (f) is preferred at high temperatures. The Andersson phases $Cr_2Ti_{n-2}O_{2n-1}$ can be obtained similarly to (f) and (g) by addition of $(n-3)$ moles $TiO_2$.

Reactions (h–k) and (q) are different reactions along the line **5**–**4c**–**3c**–**2d** (Fig. 2). In the MAT system, the phase assemblage (**2d**, **4c**) is preferred at high temperatures and (**2d**, **5**) at lower temperatures, where phase (**4**) becomes unstable. In the FAT and NCT systems, and probably at very low temperatures also in the FCT system, the solid solution (**3c**) or the coexisting phases (**3a**, **3e**) are stabilized by the crystal field effects of reaction (j). The change of coexisting phases from (**2**, **4**) to (**3**, **3′**) is very sensitive and could also be accomplished by an increased $Fe^{3+}$ content in the FAT system at 1300°C (Fig. 4). At very high temperatures, pseudobrookite (**4c**) can transform to a phase of $V_3O_5$ structure type or it can react with $TiO_2$ to the quarternary Andersson phases (**6**), (**7**), and (**8**), e.g. (reaction (q)). Quarternary phases if com-

pared to the ternary phases are stabilized by $H_{Fe}$ or $H_{Ni}$ in addition. Therefore, the solid solutions of (6) and (7) are more extended, particularly in the NCT system, and the quarternary phases, including that of the FAT system (*15*), extended to lower temperatures before decomposition.

In the MAT system with coexisting spinel (2) and pseudobrookite (4) the composition of spinel, e.g., in the three-phase triangles (2, 3, 4) and (2, 3', 4) changes to higher $M$ content, the pseudobrookite composition to lower $M$ content at decreasing temperatures (reactions (l), (m)). This can be related to the reverse stabilities of phases (2) and (4). The stability of phase (2) increases with $M$ content. It decreases in phase (4), if $M$ = Al or Cr. Crystal field effects of $M$ = Cr should increase and $Me$ = Fe in the FAT system decrease the reaction.

Similarly, reactions (n), (o), and (p) between coexisting phases (2, 3) or (3, 4) are stabilized at the left side by the counter clockwise change of conjugation lines at decreasing temperatures. Reaction (p) is shifted to the right side by $H_{Me}$ in the FAT and NAT and probably also in the FFT and NFT systems.

Three types of low-temperature phase diagrams can be predicted from crystal field effects, if they are the main contribution influencing different systems and for the case of no ordered quarternary compounds (Fig. 5). Phase diagrams of this investigation at the lower temperatures are already close to the predicted phase diagrams for the MAT, MCT, FAT, NAT, and NCT systems. The 1100°C isothermal section of the FCT system looks similar to the NAT system, but could change, if $\Delta H_{CFS} \simeq -4$ kcal/mole can shift reaction (j) to the right side. The low-temperature phase relation of $Fe_2O_3$-containing systems MFT, FFT, and NFT are more difficult to investigate by experiment because of the stability of $Fe_2TiO_5$. They are, however, of great importance for discussion of geochemical reactions, which occurred at low temperatures and long duration times, some also at hydrothermal conditions.

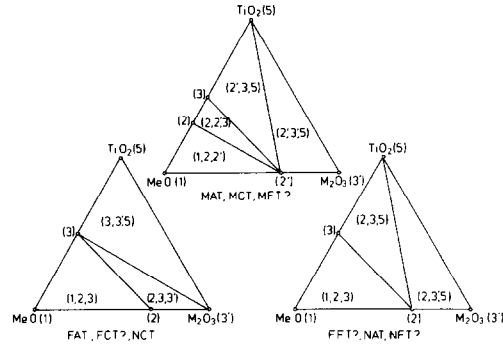


FIG. 5. Low-temperature phase diagrams for the case of no ordered quarternary compounds and for crystal field effects as the main contribution to phase relations different from that of the MAT system.

## Acknowledgment

Critical reviews by Professors P. S. Rudman (Haifa) and E. Woermann (Aachen) were helpful in improving the manuscript.

## References

1. A. MUAN, J. HAUCK, AND T. LÖFALL, *Proc. Third Lunar Sci. Conf., Geochim. Cosmochim. Acta (Suppl. 3)* **1**, 185 (1972).
2. A. MUAN, J. HAUCK, E. F. OSBORN, AND J. F. SCHAIRER, *Proc. Second Lunar Sci. Conf., Geochim. Cosmochim. Acta (Suppl. 2)* **1**, 497 (1971).
3. J. HAUCK, K. JOHANSEN, AND A. MUAN (1971), unpublished.
4. R. D. SHANNON AND C. T. PREWITT, *Acta Crystallogr. Sect. B* **25**, 925 (1969).
5. D. S. MCCLURE, *J. Phys. Chem. Solids* **3**, 311 (1957).
6. J. D. DUNITZ AND L. E. ORGEL, *J. Phys. Chem. Solids* **3**, 318 (1957).
7. D. M. ADAMS, "Inorganic Solids," Wiley, London (1974).
8. J. HAUCH, *Z. Naturforsch. B* **24**, 1347 (1969).
9. M. SAUVAGE AND E. PARTHÉ, *Acta Crystallogr. Sect. A* **30**, 239 (1974).

*10.* G. BLASSE, *Philips Res. Rep. Suppl.*, No. 3 (1964).
*11.* R. W. G. WYCKOFF, "Crystal Structures," 2nd ed., Interscience, New York (1965).
*12.* E. W. GORTER, *Proc. Int. Congr. Pure Appl. Chem.* **17**, No. I, 303 (1959).
*13.* S. ANDERSSON AND L. JAHNBERG, *Ark. Kemi* **21**, 413 (1963).
*14.* I. E. GREY AND A. F. REID, *J. Solid State Chem.* **4**, 186 (1972).
*15.* L. A. BURSILL, I. E. GREY, AND D. J. LLOYD, *J. Solid State Chem.* **16**, 331 (1976).
*16.* S. ANDERSSON AND J. GALY, *J. Solid State Chem.* **1**, 576 (1976).
*17.* C. HAAS, *J. Phys. Chem. Solids* **26**, 1225 (1965).
*18.* S. E. HAGGERTY AND D. H. LINDSLEY, *Carnegie Inst. Washington Year Book* **68**, 247 (1969).
*19.* S. SOMIYA, S. HIRANO, AND S. KAMIYA, *J. Solid State Chem.* **25**, 273 (1978).
*20.* D. H. LINDSLEY, S. E. KESSON, M. J. HARTZMAN, AND M. K. CUSHMAN, *Proc. Lunar Sci. Conf. 5th*, 521 (1974).
*21.* R. W. TAYLOR, *Amer. Mineral.* **49**, 1016 (1964).
*22.* L. M. ATLAS AND W. K. SUMIDA, *Amer. Ceram. Soc.* **41**, 150 (1958).
*23.* B. SIMONS AND E. WOERMANN, *Contrib. Mineral. Petrol.* **66**, 81 (1978).
*24.* I. E. GREY AND J. WARD, *J. Solid State Chem.* **7**, 300 (1973).
*25.* I. E. GREY, A. F. REID, AND D. G. JONES, *Trans. Inst. Miner. Metall. 83C*, 105 (1974).
*26.* I. E. GREY, C. LI, AND A. F. REID, *J. Solid State Chem.* **11**, 120 (1974).
*27.* B. KNECHT, B. SIMONS, AND E. WOERMANN, *Proc. Lunar Sci. Conf. 8th*, 2125 (1977).
*28.* E. WOERMANN, B. BREŽNY, AND A. MUAN, *Amer. J. Sci. A* **267**, 463 (1969).